Parallel gradients in comprehensive multidimensional liquid chromatography enhance utilization of the separation space and the degree of orthogonality when the separation mechanisms are correlated

Aly, A.A.; Muller, M.; de Villiers, A.; Pirok, B.W.J.; Górecki, T.

DOI
10.1016/j.chroma.2020.461452

Publication date
2020

Document Version
Final published version

Published in
Journal of Chromatography A

Journal of Chromatography A 1628 (2020) 461452

Contents lists available at ScienceDirect

Journal of Chromatography A

journal homepage: www.elsevier.com/locate/chroma

Parallel gradients in comprehensive multidimensional liquid chromatography enhance utilization of the separation space and the degree of orthogonality when the separation mechanisms are correlated

Alshymaa A. Aly[a,b], Magriet Muller[c], Andre de Villiers[c], Bob W.J. Pirok[d], Tadeusz Górecki[a,*]

[a] Department of Chemistry, University of Waterloo, Waterloo, ON, Canada
[b] Analytical Chemistry Department, Faculty of Pharmacy, Minia University, Menia Governorate, Egypt
[c] Department of Chemistry and Polymer Science, Stellenbosch University, Stellenbosch, South Africa
[d] Van 't Hoff Institute for Molecular Sciences, University of Amsterdam, Amsterdam, the Netherlands

ARTICLE INFO

Article history:
Received 30 April 2020
Revised 22 July 2020
Accepted 4 August 2020
Available online 5 August 2020

Keywords:
Comprehensive two-dimensional liquid chromatography
RPLC×RPLC
parallel gradients
orthogonality
pharmaceutical compounds

ABSTRACT

Comprehensive two-dimensional liquid chromatography (LC×LC) offers increased peak capacity, resolution and selectivity compared to one-dimensional liquid chromatography. It is commonly accepted that the technique produces the best results when the separation mechanisms in the two dimensions are completely orthogonal, which necessitates the use of gradient elution for each second-dimension fraction. Recently, the use of similar separation mechanisms in both dimensions has been gaining popularity, but full or shifted gradients are still used for each second dimension fraction. Herein, we argue that when the separation mechanisms are correlated in the two dimensions, the best results can be obtained with the use of parallel gradients in the second dimension, which makes the technique nearly as user-friendly as comprehensive two-dimensional gas chromatography. This has been illustrated through the separation of a mixture of 39 pharmaceutical compounds using reversed phase in both dimensions. Different selectivity in the second dimension was obtained through the use of different stationary phase chemistries and/or mobile phase organic modifiers. The best coverage of the separation space was obtained when parallel gradients were applied in both dimensions, and the same was true for practical peak capacity.

1. Introduction

Comprehensive two-dimensional liquid chromatography (LC×LC) is a powerful technique for the analysis of complex samples because of its ability to achieve higher peak capacities and greatly increased resolving power compared to one-dimensional liquid chromatography. The first LC×LC system was implemented by Erni and Frei [1] who analyzed a complex plant extract. In the recent years, LC×LC methods have been developed and applied among others to separate different kinds of polycyclic aromatic compounds [2], pharmaceuticals [3], proteins [4], synthetic polymers [5], natural products [6] and in proteomics [7]. Many applications have been reported in food analysis, including soybean [8], corn oil [9], wholegrain bread extracts [10] and plant extract [11]. Other applications included the determination of phenolic acids [12] and flavonoids [13]. The large number of applications demonstrates the growing interest in this technique [14].

Ever since Giddings laid the foundations for comprehensive multidimensional separations [15,16], it has been universally accepted that the best results are always obtained when the separation mechanisms used in the two dimensions are completely orthogonal, i.e. not correlated with each other. LC offers numerous separation mechanisms, including normal phase, reversed phase, ion exchange, size exclusion, affinity chromatography, etc., and all of them are characterized by different selectivity [17]. Consequently, LC×LC can in theory be deployed in a vast number of combinations [15]. However, certain LC modes cannot be easily combined due e.g. to the immiscibility of the mobile phases or the incompatibility between the mobile phase from the first dimension and the stationary phase of the second dimension [17]. In addition, the use of orthogonal separation mechanisms necessitates the use of gradient elution in the second dimension, as with no correlation between the mechanisms, it is likely that compounds that are both weakly and strongly retained in the second column may be

* Corresponding author.
E-mail address: tgorecki@uwaterloo.ca (T. Górecki).

https://doi.org/10.1016/j.chroma.2020.461452
0021-9673/

present in the same fraction. Gradient elution in the second dimension (^{2}D) is technically challenging, as it needs to happen on a time scale of a single fraction separation. It also reduces the available separation space, as the ^{2}D column must be re-equilibrated after each fraction, during which time no analyte should be eluting from it.

Comprehensive two-dimensional gas chromatography (GC×GC) offers a stark contrast to LC×LC with orthogonal separation mechanisms. In GC×GC, the separation mechanisms in the two dimensions are never fully orthogonal, as they are always at least partially correlated through analyte volatility. Simply put, it is impossible that analytes with both very low and very high volatility be present in a single fraction. While this might seem disadvantageous, GC×GC has enjoyed considerable success over the years. With analytes pre-separated based on their volatility in the first dimension, separation in the second dimension can fully explore the different selectivity of the stationary phase. Moreover, since the ^{2}D retention differences of analytes in a given fraction cannot be extreme, the separation in this dimension can be carried out under practically isothermal conditions. This makes the system overall less complicated (various issues with modulation aside). The price for this simple approach is the increased probability of peak wraparound, a phenomenon occurring when the retention time of an analyte is longer than the modulation period. Over the years, the GC×GC community has learned how to reduce the impact of wraparounds, which are considered these days more or less normal occurrence. Generally speaking, wraparounds create problems when they lead to coelutions. In all other cases, they help fill the separation space, including areas not normally accessible to separation (^{2}D retention times shorter than the dead time) [18].

The Jandera group explored the use of parallel gradients for some time now. In 2007, Cacciola et al. developed a comprehensive two-dimensional liquid chromatography system for the separation of phenolic and flavone antioxidants in beer and wine samples using reversed phase in both dimensions with parallel gradients, in which the gradient started at a low concentration of organic modifier and then this concentration increased gradually over time [19]. Afterwards, in 2008, Jandera et al. confirmed that adopting parallel gradients in the first and second dimension increased the use of the available second-dimension separation time and could remarkably boost the regularity of the coverage of the available separation space in RPLC×RPLC separations [20]. In 2009, Česla et al. developed an almost fully orthogonal LC×LC system for the separation of phenolic and flavone natural antioxidants by using reversed phase stationary phases and parallel gradients in both dimensions [21]. They demonstrated that parallel gradients in the second dimension resulted in good coverage of the 2D retention plane, and thus orthogonality. In the same year, Bedani et al. proposed a new type of ^{2}D gradient called shifted gradients, in which each individual ^{2}D gradient had a narrow range of mobile phase composition varying according to the ^{1}D retention time of compounds [22]. The main limitation of this approach was the need for specialized software to generate different ^{2}D gradients for each ^{1}D fraction; this problem was solved by Li et al. [23], who introduced software dedicated to shifted gradients in 2013. In spite of the growing popularity of shifted gradients, full gradients, in which the gradient covers a wide range of mobile-phase compositions in a very short time, are still mostly being used in numerous applications [24–27].

There is still no consensus about which type of ^{2}D gradient works the best when it comes to maximizing the utilization of the separation space, especially when the same separation mechanisms (e.g. reversed phase × reversed phase) are used in both dimensions in LC×LC systems. Shifted gradients are generally considered the best approach in the second dimension in spite of the fact that they require special software and hardware, which is not available in many laboratories. Recently, the merits and demerits of different second dimension gradient strategies have been studied by Leme et al. for the determination of the polyphenolic content of sugarcane leaves. They concluded that the use of parallel gradients was the least effective approach [28]. Herein, we argue that LC×LC can be carried out in a manner similar to GC×GC when the separation mechanisms in the two dimensions are correlated, using reversed phase LC (RPLC×RPLC) as an example. With analytes pre-separated in the first dimension based on their hydrophobicity, the second-dimension separation can be carried out practically isocratically. This can be accomplished by using simple parallel gradients. With no need to re-equilibrate the ^{2}D column after each fraction, the space available for the separation in ^{2}D increases significantly, leading to higher overall peak capacity. What is more, we argue that parallel gradients by definition lead to the best utilization of the two-dimensional separation space if compared to full or shifted gradients when the separation mechanisms are correlated. The degree of orthogonality was calculated for all proposed systems and the results proved that the highest orthogonality was achieved when parallel gradients were adopted in both dimensions.

An emulated on-line LC×LC system and a state-of-the-art online LC×LC system were used for the separation of a mixture of pharmaceutical compounds using RP mode in both dimensions, thus minimizing the mobile phase mismatch problems. The use of reversed phase in both dimensions is very advantageous because the separation efficiency is much higher than that in other modes. The conditions in both dimensions were optimized to accomplish good coverage of the separation space, which is considered a measure of orthogonality, and high peak capacity. In addition, the PIOTR program developed at the University of Amsterdam was used to simulate separations using shifted and parallel gradients. The simulation results obtained using the program confirmed that the best utilization of the separation space can be achieved when parallel gradients are used in both dimensions.

2. Experimental

2.1. Materials and reagents

HPLC grade acetonitrile, methanol and acetic acid were purchased from Sigma-Aldrich. Ultra-pure water was obtained using a Milli-Q water purification system from Millipore (Bedford, MA, USA). The pH of the mobile phase was adjusted with the help of a pH-meter (SevenEasy pH, Mettler Toledo, Switzerland). The mixture of pharmaceutical compounds used in the study contained 39 components of varying properties. It contained (1) - sulfanilamide, (2) - theophylline, (3) - sulfacetamide, (4) - caffeine, (5) - sulfadiazine, (6) - sulfathiazole, (7) - sulfapyridine, (8) - sulfamerazine, (9) - sulfamethazine, (10) - sulfamethoxypyridazin, (11) - sulfamonomethoxine, (12) - acetylsalicylic acid, (13) - sulfamethoxazole, (14) - sulfadimethoxine, (15) - sulfaphenazole, (16) - ethylparaben, (17) - propylparaben, (18) - ketoprofen, (19) - propranolol, (20) - estrone, (21) - fenoprofen, (22) - flurbiprofen, (23) - diclofenac, (24) - ibuprofen, (25) - phenylbutazone, (26) - meclofenamic acid, (27) - diflunizal, (28) - indomethacin, (29) - naproxen, (30) - sulfisomidine, (31) - sulfaisoxazole, (32) - butylparaben, (33) - nicotinamide, (34) - terbutaline, (35) - thiamine, (36) - acetaminophen, (37) - atenolol, (38) - metoprolol and (39) - nadolol. Table S1 in the supplementary information section presents the characteristics of these pharmaceutical drugs. All components were purchased from Sigma-Aldrich with purity greater than 98%. The stock solutions of these compounds were prepared by dissolving 25 mg of each standard in 10 mL purified water or methanol according to their solubility. The working standard solutions were prepared by serial dilution of the stock solutions. All solutions were stored in the dark at 4 °C.

Table 1
Experimental conditions used with setups 1–3.

Set-up	Column	^{1}D mobile phase	^{2}D mobile phase	Modulation period	^{1}D Gradient and flow rate	^{2}D gradient and flow rate
1 Parallel gradients	^{1}D column: Kinetex C18 (4.6 × 150 mm, 2.6 µm) ^{2}D column: Raptor^{TM} C18 (4.6 × 30 mm, 2.7 µm)	A: 0.5% acetic acid in H_2O B: 0.5% acetic acid in ACN	A: 0.5% acetic acid in H_2O B: 0.5% acetic acid in MeOH	0.5 min 20 µL loops	0.00 min: 10% B, ^{1}F = 0.7 mL/min 2.60 min: 11% B, ^{1}F = 0.4 mL/min 10.0 min: 11% B, ^{1}F = 0.4 mL/min 30.0 min: 36% B, ^{1}F = 0.5 mL/min 50.0 min: 75% B, ^{1}F = 0.5 mL/min	0.00 min: 2 % B 8.00 min: 10% B 34.0 min: 55% B 50.0 min: 80% B 52.0 min: 80% B ^{2}F=2.5 mL/min
2 Parallel gradients	^{1}D column: Kinetex C18 (4.6 × 150 mm, 2.6 µm) ^{2}D column: Pinnacle DB PFPP (4.6 × 30 mm, 3.0 µm	A: 0.5% acetic acid in H_2O B: 0.5% acetic acid in ACN		0.5 min 20 µL loops	0.00 min: 10% B, ^{1}F = 0.7 mL/min 2.60 min: 11% B, ^{1}F = 0.4 mL/min 10.0 min: 11% B, ^{1}F = 0.4 mL/min 30.0 min: 36% B, ^{1}F = 0.5 mL/min 50.0 min: 75% B, ^{1}F = 0.5 mL/min	0.00 min: 6 % B 8.00 min: 20% B 35.0 min: 60% B 50.0 min: 80% B 52.0 min: 90% B 53.0 min: 90% B ^{2}F=2.8 mL/min
3 Parallel gradients	^{1}D column: Kinetex C18 (4.6 × 150 mm, 2.6 µm) ^{2}D column: Pinnacle DB PFPP (4.6 × 30 mm, 3.0 µm	A: 0.5% acetic acid in H_2O B: 0.5% acetic acid in MeOH		0.5 min 20 µL loops	0.00 min: 5% B, ^{1}F = 1.0 mL/min 5.00 min: 20% B, ^{1}F = 0.4 mL/min 25.0 min: 24% B, ^{1}F = 0.8 mL/min 30.0 min: 55% B, ^{1}F = 0.8 mL/min 40.0 min: 75% B, ^{1}F = 0.8 mL/min 50.0 min: 80% B, ^{1}F = 0.8 mL/min	0.00 min: 3 % B 4.00 min: 4.5% B 5.00 min: 8 % B 15.0 min: 38% B 20.0 min: 43% B 40.0 min: 73% B 45.0 min: 78% B 50.0 min: 78% B 52.0 min: 80% B ^{2}F=2.5 mL/min

2.2. Equipment

In the emulated online LC×LC experiments (see Section 2.3 below), an Agilent model 1200 HPLC system (Agilent Technologies, Waldbronn, Germany) equipped with a micro-flow binary pump, degasser, autosampler, thermostatted column compartment and UV diode array detector was used for the separations. Agilent Chemstation Software was used for instrument control and data acquisition. The column used in the first dimension was a Phenomenex Kinetex C18 (4.6 × 150 mm, 2.6 µm particle size). The columns used in the second dimension were Restek Raptor C18 (4.6 × 30 mm, 2.7 µm particle size) or Restek Pinnacle DB PFPP (4.6 × 30 mm, 3.0 µm particle size). A Rheodyne manual sample injector (Rheodyne, USA) with a 20 µL sampling loop was used for manual injection of the fractions into the second-dimension column. The data from two-dimensional liquid chromatography runs were processed using GC Image LLC^{TM} software to generate contour plots.

In the online LC×LC experiments, a Waters Cap LC 920 autosampler connected to a 10 μL sampling loop and pump was used in the first dimension. An Agilent 1290 Infinity II binary pump and DAD detector were used in the second dimension. The first-dimension column was Zorbax SB-C18 (1.0 × 150 mm, 3.5 µm particle size), whereas the second-dimension column was Zorbax Eclipse plus C18 (3.0 × 50 mm, 1.8 µm particle size). An Agilent 2-position/8-port valve was used as the interface between the first and the second dimensions. Dilution of the fractions collected from the first dimension was performed using an Agilent 1100 isocratic pump adding a 20 µL/min flow of 0.5% acetic acid in water to a T-piece prior to the valve. MassLynx software (Waters) was used to control the Cap LC, while the rest of the setup including the valve was controlled by OpenLab CDS software (Agilent). LC Image (v2.6, GC Image LLC, Nebraska, USA) was used to construct the contour plots.

2.3. Methods

Ten experimental setups with different column combinations, mobile phases and gradients were tested in this work with the emulated on-line RPLC×RPLC system. Only eight setups will be presented in this paper, while the rest will be described in the Supplementary Information section. The chromatographic separations were carried out at 30 °C for all experimental setups. Tables 1 and 2 show the experimental conditions used, including the stationary phases, the mobile phase compositions, the gradients and the flow rates used in both dimensions for the eight setups discussed in the paper. Table S2 in the Supplementary Information section presents the experimental parameters for the other two setups.

With the emulated on-line RPLC×RPLC system, setups 1, 2, 3 and 4A-E were tested. In the first step, fractions of the effluent from the first-dimension column (10 µL injection volume) were collected at regular intervals (e.g. with 30 s modulation period, 100 fractions were collected in total). Each fraction was then diluted 1:1 with ultrapure water to reduce the elution strength of the mobile phase. To emulate on-line LC×LC separation, the separation in ^{2}D was carried out using a single continuous run. In order to do this, a manual sampling loop was installed between the pump and the ^{2}D column. The pump started, and the first fraction was manually injected (20 µL injection volume) after the time of the modulation period, for example 30 s in setup 4A. The consecutive fractions were then injected at regular intervals (every 30 s in Setup

Table 2
Experimental conditions used with setups 4A–E.

Set-up 4	Column	^{1}D mobile phase	^{2}D mobile phase	Modulation period	^{1}D Gradient and flow rate	^{2}D gradient and flow rate
(4A) Parallel gradients				0.5 min 20 µL loops		0.00 min: 0.0% B 5.00 min: 5.0% B 15.0 min: 20.0% B 20.0 min: 21.5% B 40.0 min: 51.5%B 50.0 min: 61.5% B 52.0 min: 85.0% B ^{2}F=2.5 mL/min
	^{1}D column: Kinetex C18 (4.6 × 150 mm, 2.6 µm) ^{2}D column: Pinnacle DB PFPP (4.6 × 30 mm, 3.0 µm)	A: 0.5% acetic acid in H_2O B: 0.5% acetic acid in MeOH	A: 0.5% acetic acid in H_2O B: 0.5% acetic acid in ACN		0.00 min: 5% B, ^{1}F = 1.0 mL/min 5.00 min: 20% B, ^{1}F = 0.4 mL/min 25.0 min: 24% B, ^{1}F = 0.8 mL/min 30.0 min: 55% B, ^{1}F = 0.8 mL/min 40.0 min: 75% B, ^{1}F = 0.8 mL/min 50.0 min: 80% B, ^{1}F = 0.8 mL/min	
(4B) Full gradients				2.0 min (gradient from 0–1.0 min, equilibration from 1.0–2.0 min) 20 µL loops		Gradient time: 1.00 min 0.0–1.0 min: 10–90 %B 1.0–2.0 min: 10 %B ^{2}F=2.5 mL/min
(4C) Full gradients				0.5 min (gradient from 0–0.45 min, equilibration carried out when the run was finishedas in offline mode) 20 µL loops		Gradient time: 0.45 min 0.0–0.45 min: 10–95 %B 0.45–0.5 min: 10 %B ^{2}F=2.5 mL/min
(4D) Shifted gradients				1 min (gradient from 0–0.75 min, equilibration from 0.75–1.0 min) 20 µL loops		Gradient time: 0.75 min Start percentage for first fraction: 0.00 min 2 0.75 min 42 1.00 min 3 End percentage for the last fraction: 0.00 min 52 0.75 min 92 1.00 min 53 ^{2}F=2.5 mL/min
(4E) Shifted gradients				0.5 min (gradient from 0–0.49 min, equilibration carried out when the run was finished as in offline mode) 20 µL loops		Gradient time: 0.49 min Start percentage for first fraction: 0.00 min 2% B 0.49 min 42% B 0.50 min 2.5% B End percentage for the last fraction: 0.00 min 27% B 0.49 min 67% B 0.50 min 27.5% B ^{2}F=2.5 mL/min

Table 3
Experimental conditions for online LC×LC setups.

Setup	Column	^{1}D mobile phase	^{2}D mobile phase	Modulation time	Dilution flow	^{1}D gradient and flow rate	^{2}D gradient and flow rate
(5a) Full gradients				0.5 min (gradient from 0–0.4 min, equilibrate from 0.4–0.5 min) 60 µL loops		0–10 min: 5–20 %B 10–15 min: 20–25 %B 15–30 min: 25–65 %B 30–40 min: 65–85 %B 40–45 min: 85–98 %B 45–50 min: 98 %B ^{1}F=20 µL/min	0–0.4 min: 5–90 %B 0.4–0.5 min: 5 %B ^{2}F=2.4 mL/min
	^{1}D column: Zorbax SB-C18 (1.0 × 150, 3.5 µm) ^{2}D column: Zorbax Eclipse plus C18 (3.0 × 50, 1.8 µm)	A: 0.5% acetic acid in H_2O B: 0.5% acetic acid in MeOH	A: 0.5% acetic acid in H_2O B: 0.5% acetic acid in ACN		20 μL/min 0.5% acetic acid in H_2O		
(5b) Shifted gradients				0.5 min (gradient from 0–0.4 min, equilibrate from 0.4–0.5 min) 60 µL loops		0–10 min: 5–20 %B 10–15 min: 20–25 %B 15–30 min: 25–65 %B 30–40 min: 65–85 %B 40–45 min: 85–98 %B 45–50 min: 98 %B ^{1}F=20 µL/min	Gradient time: 0.4 min Start percentage: 0–8 min: 2 %B 8–50 min: 2–42 %B End percentage: 0–8 min: 42 %B 8–50 min: 42–82 %B ^{2}F=2.4 mL/min
(5c) Parallel gradients				0.5 min 60 µL loops		0–10 min: 5–20 %B 10–15 min: 20–25 %B 15–30 min: 25–65 %B 30–40 min: 65–85 %B 40–45 min: 85–98 %B 45–50 min: 98 %B ^{1}F=20 µL/min	0–8 min: 0 %B 8–30 min: 0–28 %B 30–50 min: 28–65 %B ^{2}F=2.4 mL/min
(5d) Full gradients				1 min (gradient from 0–0.6 min, equilibrate from 0.6–1 min) 80 µL loops		0–10 min: 5–20 %B 10–15 min: 20–25 %B 15–30 min: 25–65 %B 30–40 min: 65–85 %B 40–45 min: 85–98 %B 45–50 min: 98 %B ^{1}F=20 µL/min	0–0.6 min: 5–90 %B 0.6–1 min: 5 %B ^{2}F=2.4 mL/min
(5e) Shifted gradients				1 min (gradient from 0–0.6 min, equilibrate from 0.6–1 min) 80 µL loops		0–10 min: 5–20 %B 10–15 min: 20–25 %B 15–30 min: 25–65 %B 30–40 min: 65–85 %B 40–45 min: 85–98 %B 45–50 min: 98 %B ^{1}F=20 µL/min	Gradient time: 0.6 min Start percentage: 0–8 min: 2 %B 8–50 min: 2–42 %B End percentage: 0–8 min: 42 %B 8–50 min: 42–82 %B ^{2}F=2.4 mL/min
(5f) Parallel gradients				0.25 min 40 µL loops		0–10 min: 5–20 %B 10–15 min: 20–25 %B 15–30 min: 25–65 %B 30–40 min: 65–85 %B 40–45 min: 85–98 %B 45–50 min: 98 %B ^{1}F=20 µL/min	0–8 min: 0 %B 8–22 min: 0–19 %B 22–50 min: 19–72 %B ^{2}F=2.4 mL/min

Table 4
Estimated orthogonality metrics and practical peak capacities of the LC×LC setups tested.

Setup	^1n_c	^2n_c	$n_{c,2D}$	^1t_g(min)	^1t_s(min)	β	$Orth_{Vec}$	$Orth_{CH}$	$Orth_{Ast}$	$n'_{c,2D}$
Setup 1	142	18.1	2565	47.2	0.5	2.92	0.76	0.78	0.60	678
Setup 2	142	13.7	1934	47.2	0.5	2.92	0.90	0.89	0.73	594
Setup 3	125	13.6	1693	43.2	0.5	2.83	0.80	0.90	0.74	510
Setup 4A	125	14.3	1777	43.2	0.5	2.83	0.77	0.73	0.74	471
Setup 4B	125	35.8	4464	43.2	2	10.62	0.44	0.48	0.41	192
Setup 4C	125	21.2	2639	43.2	0.5	2.83	0.59	0.68	0.51	595
Setup 4D	125	19.7	2457	43.2	1	5.38	0.61	0.67	0.66	292
Setup 4E	125	12.9	1608	43.2	0.5	2.83	0.67	0.57	0.57	353
Setup 5a	137	52.8	7234	45	0.5	2.96	0.23	0.22	0.34	548
Setup 5b	137	46.0	6302	45	0.5	2.96	0.41	0.37	0.46	831
Setup 5c	137	33.9	4644	45	0.5	2.96	0.75	0.55	0.69	1017
Setup 5d	137	76.4	10,467	45	1	5.66	0.26	0.22	0.37	447
Setup 5e	137	60.2	8247	45	1	5.66	0.43	0.38	0.47	585
Setup 5f	137	22.3	3055	45	0.25	1.71	0.77	0.69	0.92	1296

Orth are orthogonality values determined using the vector (Vec), convex hull (CH) and asterisk (Ast) methods.
^1n_c and ^2n_c are the peak capacities of the ^{1}D and ^{2}D separations.
$n_{c,2D}$ is the theoretical 2D peak capacity.
β accounts for ^{1}D undersampling according to this equation [40]: $\beta\sqrt{1+3.35(\frac{^1t_s\cdot{}^1n_c}{^1t_g})^2}$.
^1t_s is the sampling time.
^1t_g is the ^{1}D gradient time.
$n'_{c,2D}$ is the practical peak capacity taking into account ^{1}D undersampling and surface coverage calculated as the average of the values determined using the vector and convex hull methods: $n'_{c,2D}=\frac{^1n_c\cdot{}^2n_c\cdot f_c}{\beta}$ [32].

4A) into the flowing stream of the mobile phase. In this way, the second-dimension separation was completed in exactly the same time as the first-dimension separation, illustrating the potential of using the method in an on-line fashion. The UV diode array detector was set to 272 and 254 nm to monitor the compounds in the effluent from the ^{2}D column. After the end of each run, the columns were equilibrated with the initial mobile phase composition for 15 min.

With the on-line RPLC×RPLC system, six setups (5a – f) were tested. The same stationary and mobile phases were used in all experiments, and three types of gradients in the second dimension (parallel, shifted and full) were tested. As a result, the modulation period varied depending on the time required to re-equilibrate the ^{2}D column. All the experimental conditions, including the stationary phases, the mobile phase compositions, the gradients and flow rates used in both dimensions are listed in Table 3.

In setups 5a – f, the effluent from the ^{1}D column was diluted on-line 1:1 with 0.5% acetic acid, collected automatically via a 2-position/8-port valve and then injected into the second dimension.

3. Evaluation of the performance of the systems

Two common metrics used to characterize the performance of LC×LC systems are the degree of orthogonality of the separation and the practical peak capacity. Numerous approaches have been proposed in the literature to estimate the orthogonality of 2D chromatographic methods, and there is no consensus with regard to which method performs the best. This makes comparison between reported orthogonality values challenging. Herein, the degree of orthogonality of each LC×LC setup was calculated using three different metrics: the vector method reported by Schmitz and coworkers [29], the convex hull method [30] and the asterisk method [31]. The first two of these methods measure the portion of the 2-dimensional space which is accessible to analytes (the surface coverage, f_c), while the asterisk method uses a set of equations that estimate orthogonality based on the distances of experimental retention times from four lines bisecting the separation space. Each of these methods was used to compare the performance of LC×LC separations using different types of gradients in the second dimension. As orthogonality values obtained using each of these methods were generally similar, especially in the case of the two metrics measuring f_c (see Table 4), the following discussion will be based mainly on orthogonality values obtained using the vector method.

The practical peak capacity of a 2D separation provides another good metric to evaluate the performance of a 2D separation system. While the theoretical 2D peak capacity is simply the product of the peak capacities of the individual dimensions, practical peak capacity also takes into account undersampling of the first dimension and the utilization of the separation space. The equations used to calculate the practical peak capacity are shown in the footnote of Table 4.

4. Results and discussion

In LC×LC, separation selectivity is determined by the stationary and mobile phases used in the first and the second dimensions. Mobile phase compatibility and its effect on the fraction transfer between the two dimensions should be considered when developing a new LC×LC system. In this study, an RPLC×RPLC system was used to avoid mobile phase incompatibility issues. Ten different emulated online LC×LC setups were tested for the separation of a mixture of pharmaceutical compounds with different combinations of columns and mobile phases. Six setups using parallel gradients in the first and the second dimension were tested in all, but only four of them will be presented in this paper. Two setups adopted full gradients, whereas the other two setups applied shifted gradients in the second dimension. In all setups, the stationary phase used in the first dimension was Kinetex C18. The stationary phases used in the second dimension were either C18 or PFPP (pentafluorophenyl propyl) using different mobile phase organic modifiers (acetonitrile or methanol). The conditions are summarized in Tables 1 and 2. Another six online LC×LC setups were tested for the separation of the same mixture using Zorbax SB-C18 column (1 × 150 mm, 3.5 µm) in the first dimension, and Zorbax Eclipse plus C18 column (3 × 50 mm, 1.8 µm) in the second dimension. The conditions are summarized in Table 3.

Fig. 1 illustrates 2D separation obtained using the same stationary phase chemistry in both dimensions (C18), but different organic modifiers. In spite of the minor difference between the two dimensions, the coverage of the separation space was reasonably good, especially at longer retention times. The calculated surface coverage of this system was 0.76 using the vector method and 0.78

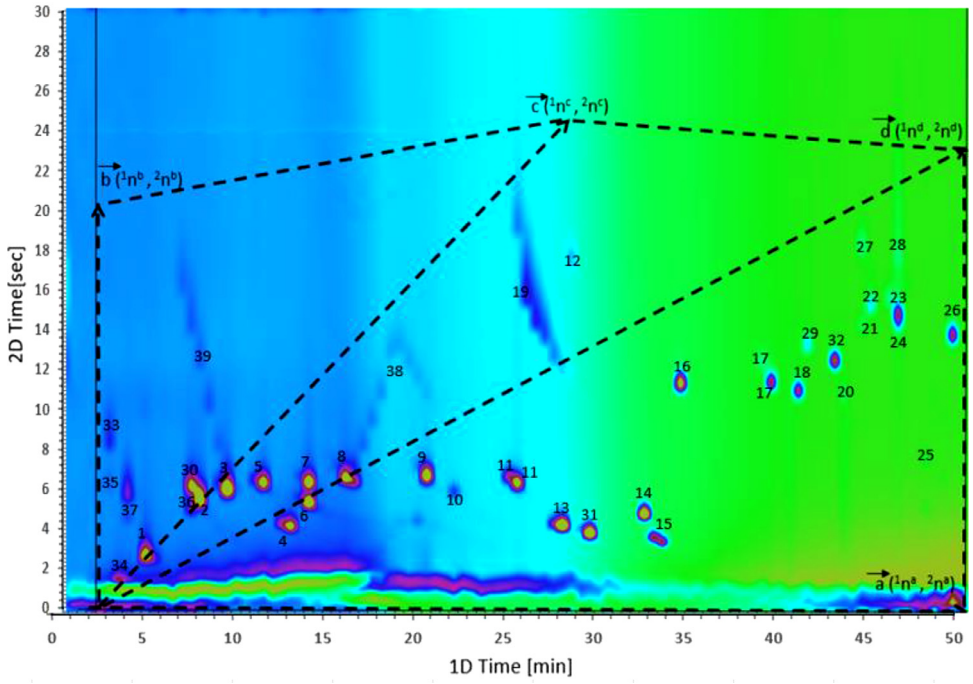

Fig. 1. Comprehensive LC×LC separation of the mixture of pharmaceutical compounds using setup 1 (parallel gradients, same stationary phase chemistry in both dimensions, different organic modifiers: ACN in ^{1}D, MeOH in ^{2}D). The modulation time was 30 s.

using the convex hull method, as shown in Table 4. This reasonably high value was obtained thanks to the good distribution of compounds in the separation space achieved by using parallel gradients in both dimensions. With parallel gradients, analytes elute from the second dimension under nearly isocratic conditions, maximizing peak resolution in the second dimension (assuming no undue peak broadening) and the coverage of the separation space. The gradual increase in the elution strength of the ^{2}D mobile phase manifests itself through the characteristic shape of tailing bands (see e.g. analyte 19). Also, because of software limitations, some of the peaks split between two fractions were not properly combined into a single peak; analyte numbers are repeated twice in such cases. This limitation could be overcome by using a selective detector (e.g. MS), which would facilitate identification of analytes in the individual fractions, or by using a shorter modulation period resulting in smaller differences between analyte retention times in consecutive fractions. Very short modulation periods can be easily accomplished with parallel gradients (as will be shown below), but are not practical using any kind of repetitive gradients in the second dimension. Overall, Fig. 1 illustrates the flexibility of the system, where different selectivity can be easily obtained simply by changing the organic phase modifiers.

Fig. 2 illustrates the separation obtained using Setup 2, with different stationary phase chemistries and organic modifiers in both dimensions (ACN in ^{1}D, MeOH on ^{2}D). This chromatogram illustrates the great potential of the approach proposed. It shows practically complete coverage of the separation space (f_c = ~0.9 using both vector and convex hull methods), indicating excellent orthogonality. Some peak wraparounds are evident (e.g. peak no. 33), but they do not interfere with the separation of other analytes.

Fig. 3 illustrates the separation obtained using Setup 3, with different stationary phases, but the same organic modifier in both dimensions (MeOH). It is quite evident that the use of the same organic modifier in both dimensions led to a slight increase in peak wraparound compared to the previous setup, but the coverage of the separation space remained good (f_c = 0.80 and 0.90 calculated by vector and convex hull methods, respectively).

In Setup 4, different types of gradients were adopted in the second dimension to compare the effect of gradient type on the distribution of compounds in the second dimension and so the coverage of the separation space. In all subcategories of setup 4, the difference in the degree of orthogonality calculated for each system proved that the maximum utilization of the retention space was achieved when parallel gradients were used. Fig. 4A illustrates the separation obtained using different stationary phase chemistries and organic modifiers in both dimensions (MeOH in ^{1}D, ACN in ^{2}D), and parallel gradients in the second dimension (Setup 4A). The chromatogram shows very good coverage of the separation plane (f_c = 0.77 and 0.73 calculated by the vector and the convex hull methods, respectively), indicating good orthogonality. As the ^{2}D column did not need to be re-equilibrated before the injection of the next fraction, the second dimension time was used efficiently.

On the other hand, it should be pointed out that any kind of repetitive gradient in the second dimension leads to the reduction of the separation space accessible to the analytes. Setup 4B, in which the same stationary and mobile phases were used as in setup 4A, but full gradients were applied in ^{2}D, will be used as an example. The modulation period in this setup was 120 s to provide sufficient time to re-equilibrate the ^{2}D column. Since the same separation mechanism (reversed phase) was used in both dimensions, analytes that were weakly retained in ^{1}D, thus eluting early from this dimension, tended to also elute early from ^{2}D, and vice versa. As a result, all analytes would fall along a diagonal line, which is a hallmark of non-orthogonality as shown in Fig. 4B (the f_c value was 0.44 and 0.48 calculated by the vector and the convex hull methods, respectively). Moreover, the ^{1}D fractions collected every 120 s contained larger numbers of compounds compared to the fractions collected every 30 s in setup 4A. This led to numerous analyte coelutions caused by re-mixing of components already separated in ^{1}D, exacerbated by the fact that the steep gradient of the mobile phase used in ^{2}D resulted in poor resolution of peaks in this dimension. Finally, it should be emphasized that only about half of the total ^{2}D cycle time was devoted to analyte separation,

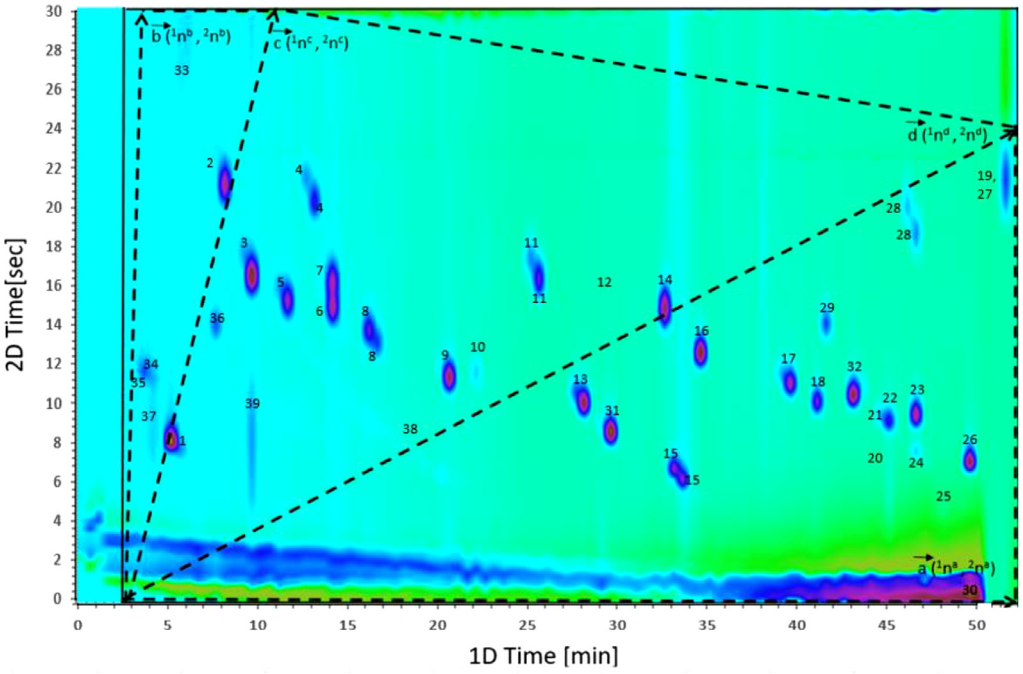

Fig. 2. Comprehensive LC×LC separation of the mixture of pharmaceutical compounds using setup 2 (parallel gradients, different stationary phase chemistries, ACN in ^{1}D, MeOH in ^{2}D). The modulation time was 30 s.

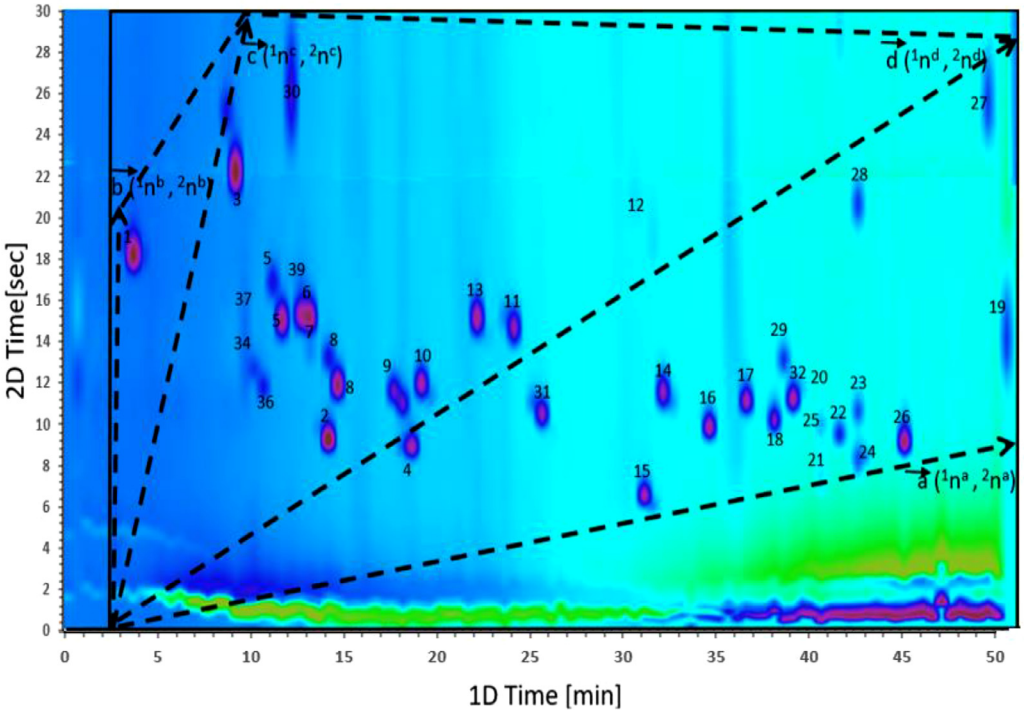

Fig. 3. Comprehensive LC×LC separation of the mixture of pharmaceutical compounds using setup 3 (parallel gradients, different stationary phase chemistries, MeOH in ^{1}D and ^{2}D). The modulation time was 30 s.

with the rest spent on column re-equilibration. This leads to very inefficient use of the total separation time.

In setup 4C, we emulated a 30 s modulation period in an RPLC×RPLC system using full gradients in the second dimension, and calculated the degree of orthogonality of this system (Fig. 4C). In reality, 30 s modulation with full gradients in ^{2}D would be very difficult to accomplish with a conventional HPLC instrument, hence this separation was performed in an offline mode. 30 s fractions of the ^{1}D effluent were first collected and diluted 1:1 with water. Each fraction was then subjected to 30 s ^{2}D separation carried out off-line. The ^{2}D column was re-equilibrated before injecting the next fraction. The re-equilibration time was ignored during data processing. The average f_c for this hypothetical system calculated by the vector and the convex hull methods was 0.64, indicating that even if full gradients in ^{2}D could be accomplished using very short modulation periods on state-of-the-art UHPLC instrumenta-

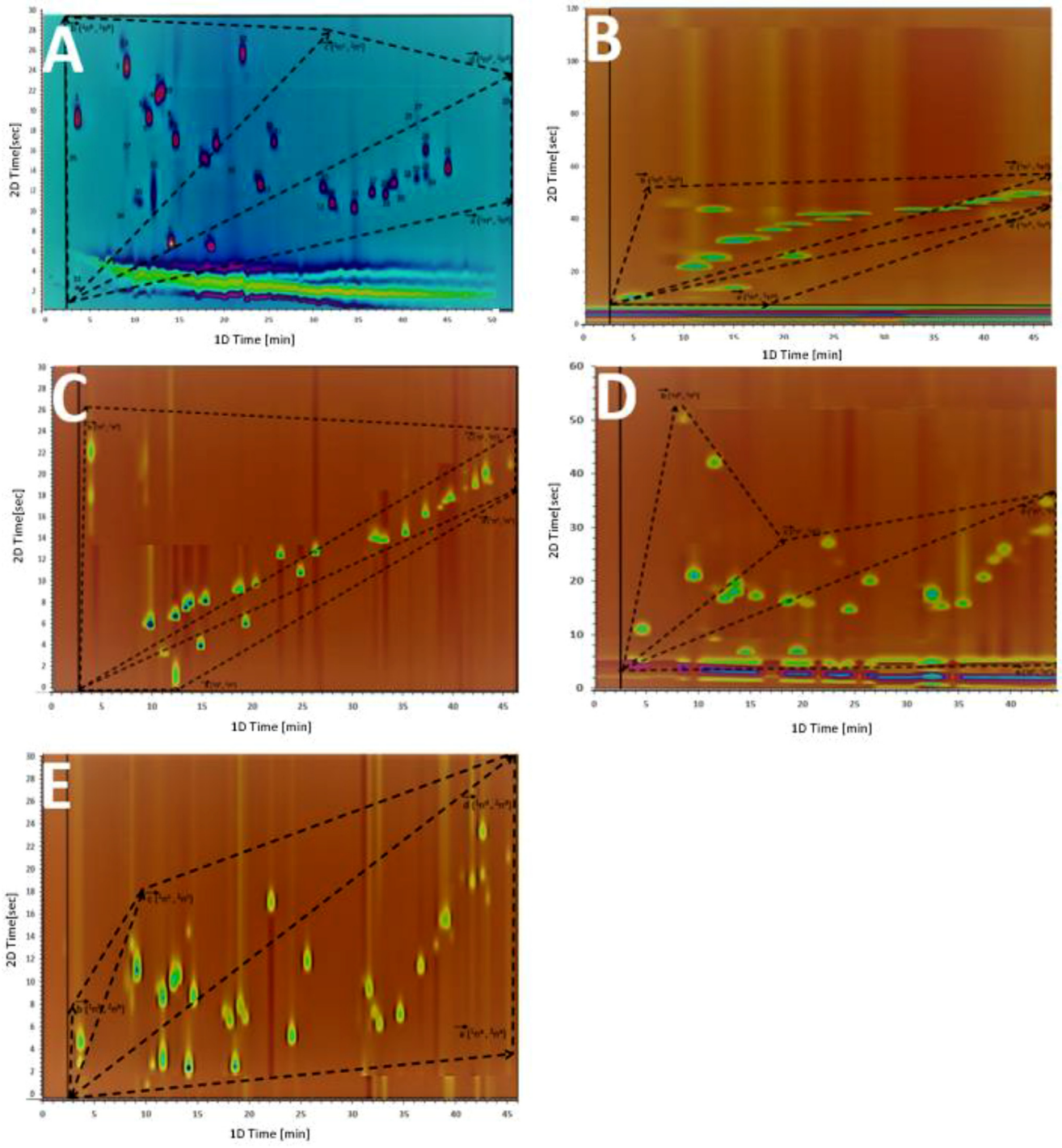

Fig. 4. Comprehensive LC×LC separation of the mixture of pharmaceutical compounds using different stationary phase chemistries, MeOH in ^{1}D and ACN in ^{2}D. (A) setup 4A: modulation time 30 s, parallel gradients; (B) setup 4B: modulation time 120 s, full gradients used in ^{2}D; (C) setup 4C: modulation time 30 s, full gradients used in ^{2}D; (D) setup 4D: modulation time 60 s, shifted gradients used in ^{2}D; (E) setup 4E: modulation time 30 s, shifted gradients used in ^{2}D.

tion (refer to the discussion on setups 5a-f below), better utilization of the separation space would still be achieved with parallel gradients in both dimensions.

In setup 4D, shifted gradients were used in the second dimension. The modulation period in this setup was 60 s to provide sufficient time to re-equilibrate the ^{2}D column to the initial conditions of the next fraction. As shown in Fig. 4D, the coverage of the separation space was better than in Fig. 4B when full gradients were used, but still worse than in Fig. 4A when parallel gradients were used. With shifted gradients, each fraction would be subject to too low elution strength at the beginning, and too high elution strength at the end. Thus, less retained compounds in each fraction would elute slightly later, while more retained ones slightly earlier, leading to overall compression of the band of analytes and reducing the resolution in the second dimension. The average of the f_c values calculated by the vector and the convex hull methods of this setup was 0.64.

In setup 4E, we emulated 30 s modulation period with shifted gradients in the second dimension and calculated the degree of orthogonality of this system. This experiment was again carried out

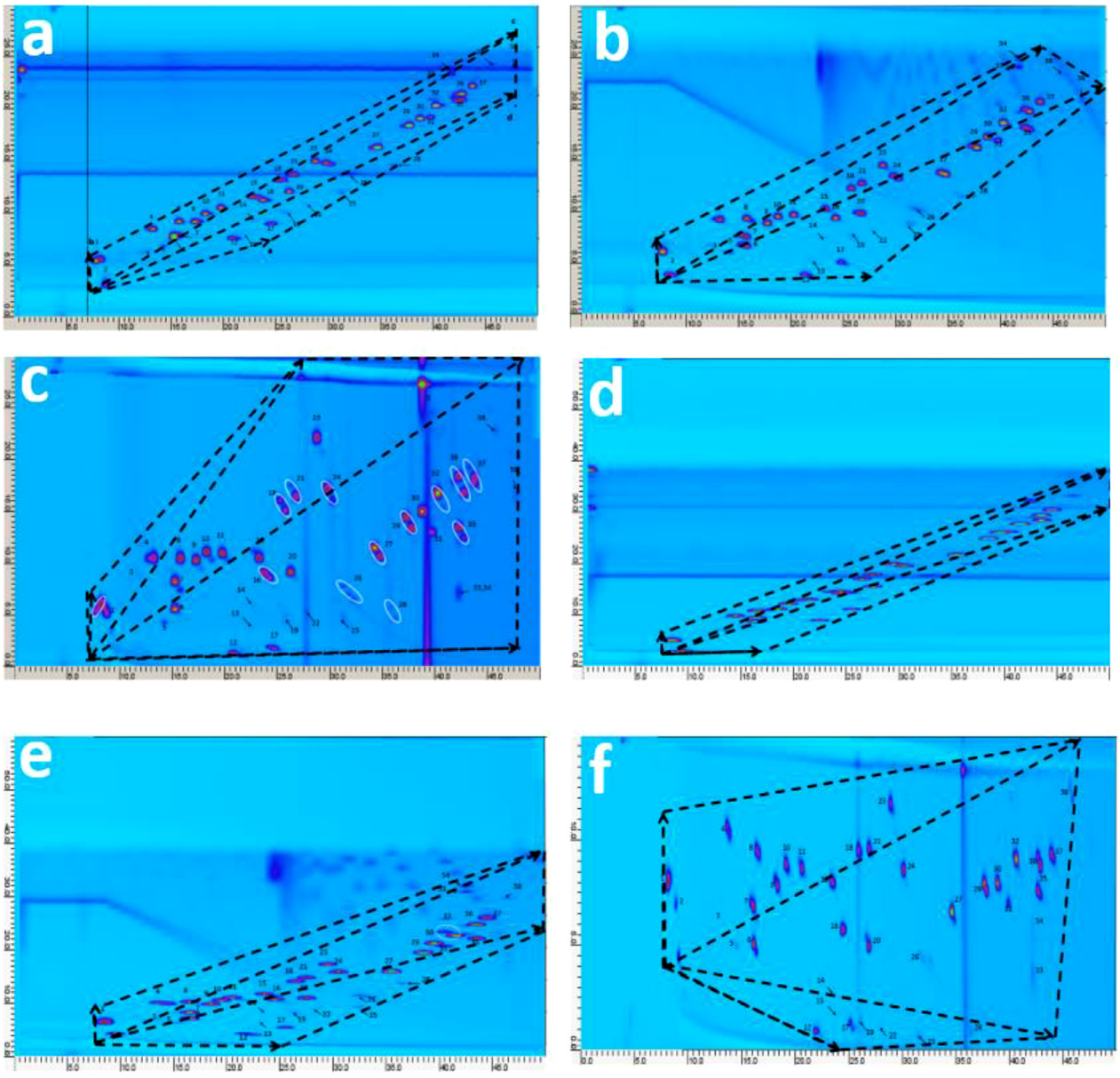

Fig. 5. Comprehensive online LC×LC separation of the mixture of pharmaceutical compounds using C18 stationary phases in both dimensions and different organic modifiers (MeOH in ^{1}D, ACN in ^{2}D) (a) setup 5a: modulation time 30 s; full gradients used in ^{2}D; (b) setup 5b: modulation time 30 s; shifted gradient used in ^{2}D; (c) setup 5c: modulation time 30 s; parallel gradients; (d) setup 5d modulation time 60 s, full gradients used in ^{2}D; (e) setup 5e: modulation time 60 s, shifted gradient used in ^{2}D; (f) setup 5f: modulation time 15 s, parallel gradients.

in offline mode. Fractions of ^{1}D effluent collected every 30 s were separated in the second dimension in 30 s. The run was stopped and the ^{2}D column was re-equilibrated before injecting the next fraction. As before, the re-equilibration time was ignored during data processing. The average of the f_c values calculated by the vector and the convex hull methods was 0.62 (Fig. 4E). When comparing setups 4A, 4C and 4E, which all used the same gradient time, it is clear that the surface coverage, hence orthogonality, increased in the order full gradients < shifted gradients < parallel gradients, indicating again that the best utilization of the separation space and the best resolution of peaks in LC×LC systems with correlated separation mechanisms in the two dimensions can be achieved when parallel gradients are used. Figs. S1 and S2 in the Supplementary Information section illustrate the separations obtained using the remaining two emulated online LC×LC setups.

The experiments described thus far were carried out using standard HPLC instrumentation, which can be easily adopted to on-line LC×LC using parallel gradients, but is not suitable for LC×LC separations using full or shifted gradients in ^{2}D with short gradient times (e.g. 30 s as in setups 4C and 4E). However, this is possible with modern, dedicated LC×LC instrumentation, hence it was important to verify whether the conclusions from the study applied also when such instrumentation was used. It is for this reason that similar experiments were carried out on an Agilent 1290 dedicated LC×LC system. Since these experiments (setups 5 a-f) were carried out in a different laboratory, the stationary phases used in the two dimensions were different than in the original study. Nevertheless, the conclusions are still applicable. Table 4 summarizes the results obtained using the on-line system. The noticeably higher 2D peak capacities measured for setups 5 a-f were a consequence

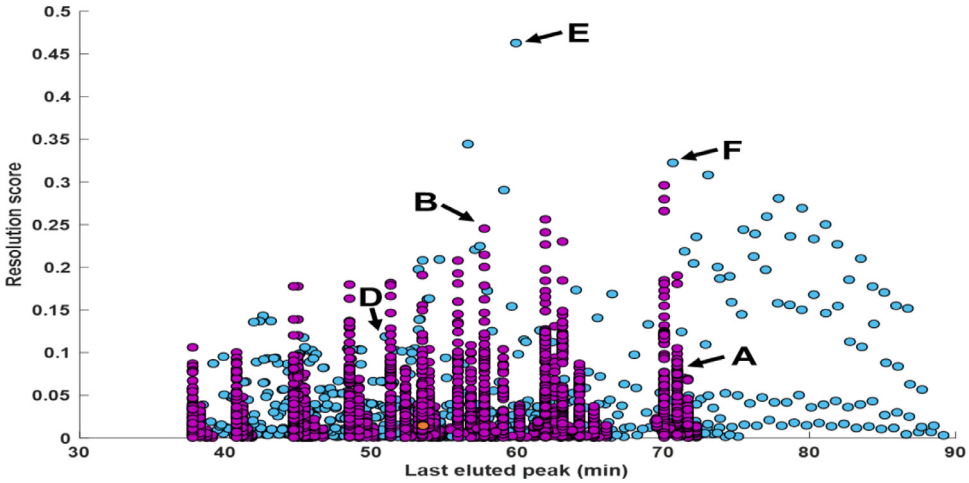

Fig. 6. Pareto-optimality plot showcasing all 25,240 simulations carried out in this study. The blue points represent simulations of parallel gradients, whereas the purple points represent simulations from experiments using shifted gradients. The symbols refer to the corresponding simulated 2D-LC chromatograms shown in Fig. 7. The orange data point represents chromatogram C from Fig. 7. (For interpretation of the references to color in this figure legend, the reader is referred to the web version of this article.)

of the smaller particle size of the ^{2}D column used in these experiments, and the use of a dedicated UHPLC instrument with reduced extra-column volume and a fast DAD detector. The experiments confirmed that parallel gradients in the second dimension provided very good coverage of the separation plane, leading to better orthogonality compared to full or shifted gradients, as shown in Fig. 5a-f. The highest surface coverage was obtained with setups 5c (0.65) and 5f (0.73), in which parallel gradients were used in both dimensions. This confirms the conclusions from the experiments carried out using the emulated on-line system.

Setup 5f deserves particular attention. In this setup, the modulation period was only 15 s, which is very uncommon in LC×LC separations. Such a short modulation period was possible because of the use of parallel gradients in both dimensions, which do not necessitate column re-equilibration before the injection of each fraction. This setup produced clearly superior results approaching the quality of GC×GC separations, with minimal ^{1}D undersampling and the highest surface coverage and peak capacity of all the setups tested.

In addition to orthogonality evaluation through surface coverage determined using the vectors and the convex hull methods, Table 4 also reports orthogonality estimates obtained using the asterisk equation. As mentioned before in Section 3, this method estimates orthogonality based on the distances of experimental retention times from four lines bisecting the separation space, hence rather than focusing on surface coverage, it looks for the undesirable clustering of peaks. The results obtained using this method confirmed the conclusions drawn based on the two other methods. As before, the highest degree of orthogonality was achieved when parallel gradients were used in both dimensions. The calculated orthogonality was 0.74 for the emulated online setup 4A, 0.69 for the online LC×LC setup 5c using 30 s modulation period, and 0.92 for the online LC×LC setup 5f using the modulation period of 15 s.

Another very useful metric used to characterize the performance of an LC×LC system is the practical 2D peak capacity [29]. It depends not only on the degree of orthogonality, but also on the undersampling of ^{1}D peaks [32]. Table 4 shows the practical peak capacities for all setups using the average f_c values determined using the vector and convex hull methods. Also in this case, the performance of the system was the best when parallel gradients were used in both dimensions. The practical peak capacity reached a maximum value of nearly 1300 in the on-line system when the sampling time was 15 s in setup 5f, compared to ~1000 when the sampling time was 30 s (setup 5c). The 15 s sampling time is only practical with parallel gradients, as there is no need to re-equilibrate the column after the separation of each fraction. Decreasing the sampling time thus enhances the practical peak capacity and improves the resolution of peaks.

5. PIOTR model

PIOTR is a program developed at the University of Amsterdam for interpretive optimization of two-dimensional resolution [33]. It facilitates rapid development of LC×LC methods. Using input data from chromatograms recorded under specific, known conditions, the program can model retention of the analytes in a given chromatographic system as a function of the mobile phase composition. The graphical interface of the software is shown in Fig. S3 in the Supplementary Information section.

In this study, chromatograms were recorded using three different gradient elution programs for two stationary phase systems that were used in the first and second dimensions in the offline and online setups. One of them was a Phenomenex Kinetex C18 column (150 × 4.6 mm, 2.6 μm), and the other one was a Restek Pinnacle DB PFP column (30 × 4.6 mm, 3 μm). To determine the retention parameters of these two systems, the method and system information were supplied to the program. The dwell volume was assumed to be roughly 1.0 mL. The resulting retention parameters were recorded for all analytes in both chromatographic systems. Retention curves for each analyte were then plotted.

Having established the retention behavior of all analytes, the two individual sets were combined to allow hypothetical prediction of retention in an LC×LC system. Due to the fact that the physical dimensions of both columns were different (150 × 4.6 mm and 30 × 3.0 mm for the C18 and PFP column, respectively), the dead volumes for all following LC×LC predictions were adjusted to reflect those of 150 × 1.0 mm and 50 × 3.0 mm columns, respectively. This was possible because the retention parameters are independent of the physical column dimensions as long as the stationary phase material is identical. The efficiency of the columns is expected to be different, but this should mainly affect peak shapes rather than the location of the peaks in the retention space.

Using the PIOTR interface, 24,000 different regular shifted gradients, and 1240 parallel gradients were simulated. In the case of the shifted gradients, the total number of gradient assemblies possible was the product of all of the steps per parameter (i.e. 5 × 4 × 4 × 3 × 5 × 5 × 4 = 24,000 different methods). Tables S3 and S4 in the supplementary information section show the

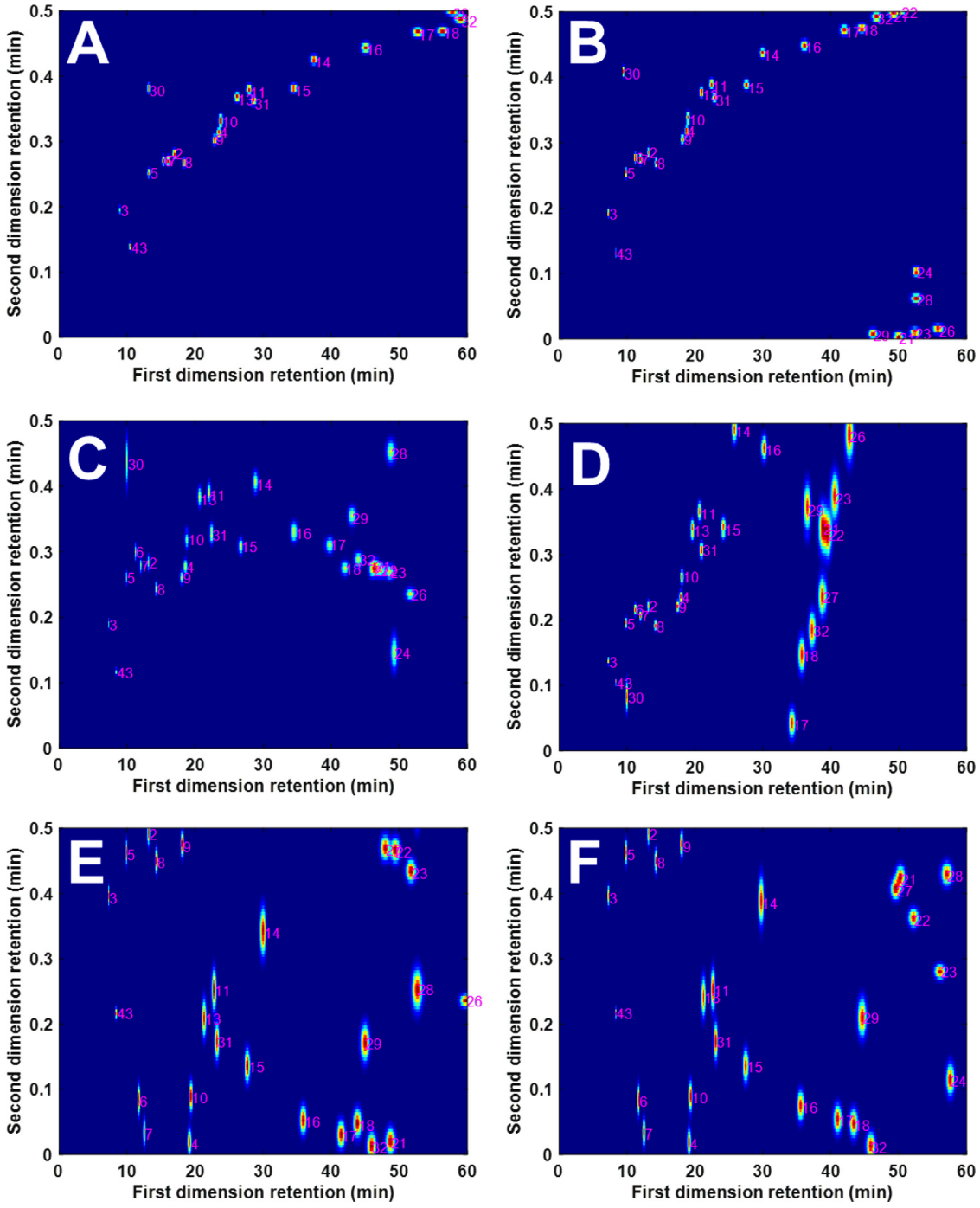

Fig. 7. Simulated LC×LC separations of the analyte mixture using different forms of mobile-phase composition programs. Figures A and B used shifted gradients, while C, D, E, and F used parallel gradients.

method parameter ranges used for the prediction of 24,000 shifting gradients and 1240 parallel gradients. The modulation time in all simulations was set to 0.5 min, as this was the modulation period already used in the experiments. The length of the boundary gradients was defined as 60 min minus the dead time of the first dimension = 56 min. The flow rate in the first dimension was set to 0.02 mL/min, and in the second dimension to 2.4 mL/min. Using just one processor on a regular computer, PIOTR required about 7 min to simulate 24,000 LC×LC methods with these analytes.

For each simulated chromatogram, the algorithms calculated the performance parameters and separation quality criteria. These can be presented in what is called a Pareto-optimal plot, in which two or more objective criteria are plotted against each other. In this plot, the analysis times (defined as the retention times of the last eluting peak) are plotted against the two-dimensional resolution. For each chromatogram, the resolution of each peak with each of its neighbors was calculated by using the metric introduced by Schure et al. [34]. The resolution was then normalized to a value between 0 and 1 by using a Derringer desirability function [35–37]. In this case, the desirability function was:

$$d\left(Rs_{i,j}\right)\begin{cases}\frac{Rs_{i,j}}{1.5} & if\ Rs_{i,j} < 1.5\\ 1 & if\ Rs_{i,j} \geq 1.5\end{cases} \quad (1)$$

Where $Rs_{i,j}$ is the resolution between peaks i and j, and $d(Rs_{i,j})$ is the desirability function that varies between 0 (complete overlap) and 1 (no overlap, i.e. resolution 1.5 or higher). Note that the equation above has a ceiling. It considers that a resolution of 1.5 is satisfactory and that it is not worth it to put extra effort into separating peaks *i* and *j* further when such a resolution is achieved. Finally, the algorithm was set to take the product of all obtained resolution values to assess the overall separation quality, O_{R_S} where m is the total number of compounds considered.

$$O_{Rs} = \Pi_{i>j}^{m} \Pi_{j=1}^{m} d\left(Rs_{i,j}\right) \quad (2)$$

In the software tool, individual points can be selected in the interactive plot shown in Fig. 6. Several have been selected and their corresponding simulated contour plots are shown in Fig. 7. Fig. 7A and 7B illustrate the results for two different generic shifting gradient assemblies. For 7A, the ^{1}D gradient ran from 15% to 80% MeOH in 60 min, whereas that in the ^{2}D varied from 15 to 85% (initially) to 25–100% MeOH (at the end). For 7B, the ^{1}D gradient ran from 20% to 90 MeOH in 60 min, while in the ^{2}D it varied from 15 to 70% (initially) to 35–100% MeOH (at the end). In both cases, the separation space was underused.

Fig. 7C shows the separation using parallel gradients with the ^{1}D gradient running from 20% to 90% MeOH in 45 min, and the ^{2}D one from 10% to 85% MeOH in 56 min. This set of very simple, nearly perfectly parallel gradients (when correcting the ^{2}D gradient for the dead time), already resulted in a major improvement in the utilization of the separation space. In this separation, even though the separation of each fraction in the second dimension was carried out under essentially isocratic conditions, peak wraparound was not present. However, if wraparound is mildly allowed, such as shown in Fig. 7D, then the separation space is utilized even more efficiently. For this experiment, the ^{1}D gradient ran from 20% to 95% MeOH in 35 min and the ^{2}D from 20% to 75% MeOH in 56 min. Peak wraparound is normally considered an undesirable phenomenon, and most LC×LC practitioners try to avoid it. However, as GC×GC chromatographers have demonstrated numerous times, wraparound is only detrimental to the separation when it leads to coelutions with components of successive fractions. If coelutions can be avoided, wraparound often leads to more efficient utilization of the separation space. Fig. 7E and 7F display the results of simulations where wraparound was strongly encouraged. In fact, both reflect Pareto-optimal points according to the plot in Fig. 6. Here, the full separation space was effectively utilized. The simulation in 7E used parallel gradients with the ^{1}D gradient running from 20% to 70% MeOH in 35 min and the ^{2}D gradient from 5% to 75% MeOH in 56 min. For 7F, the ^{1}D gradient ran from 20% to 65% MeOH in 30 min, and the ^{2}D from 5% to 75% MeOH in 56 min.

Overall, the simulation results illustrated in Fig. 6 show that in many cases parallel gradients can produce results as good as shifted gradients in comparable time, while being achievable using much simpler setups. The best results overall were obtained with parallel gradients allowing for peak wraparound, which led to the best use of the available separation space.

6. Conclusions

It is not necessary to have completely different separation mechanisms in the first and second dimensions to have a good LC×LC system. The degree of orthogonality between both dimensions is an important factor, but it is not sufficient to evaluate the full potential of a given system [38]. In Giddings's intent in the definition of orthogonality, full orthogonality implies that the separation space must be fully accessible [39]. In the RPLC×RPLC systems developed, partial or full surface coverage could be achieved through various combinations of stationary and mobile phase chemistries. Using different columns, organic modifiers and different gradients in each dimension increased the dissimilarity of the two dimensions and enhanced the orthogonality of the system. The potential of the systems was maximized in each case through the use of parallel gradients, which led to nearly-isocratic elution conditions for each fraction in the second dimension. When two-dimensional parallel gradients are adopted, simultaneous increase in the elution strength in the two dimensions with correlated retention makes it possible for the analytes in a given fraction to be eluted without using repetitive gradients in ^{2}D. With the analytes pre-separated according to their hydrophobicity in ^{1}D, the second dimension can better explore the specific interactions between the analytes, the stationary phase and the mobile phase. This decreases the correlation between the two dimensions, leading to better coverage of the retention space and hence higher orthogonality. In addition, the use of parallel gradients eliminates the need for repeated ^{2}D column re-equilibration, which results in more efficient utilization of the cycle time. This, in turn, increases the available separation space, and the practical peak capacity. Without the need to run repeated gradients in ^{2}D, the approach proposed makes it possible to perform LC×LC separations using simpler instrumentation and software, making the technique more user-friendly. It also shows how the ^{2}D separation space can be maximized when the separation mechanisms are correlated. The hypothesis that the best utilization of the separation space when using similar separation mechanisms in both dimensions can be accomplished with parallel gradients was not only confirmed through experimentation, but also through the results of simulations using the PIOTR program.

Declaration of Competing Interest

The authors declare that they have no known competing financial interests or personal relationships that could have appeared to influence the work reported in this paper.

Acknowledgments

The Egyptian government is gratefully acknowledged for the financial support of A.A. Aly. The authors would like to thank Minia University, Egypt. NSERC is gratefully acknowledged for the financial support of this research.

Supplementary materials

Supplementary material associated with this article can be found, in the online version, at doi:10.1016/j.chroma.2020.461452.

References

[1] F. Erni, R.W. Frei, Two-dimensional column liquid chromatographic technique for resolution of complex mixtures, J. Chromatogr. A 149 (1978) 561–569.
[2] R. Græsbøll, H.-.G. Janssen, J.H. Christensen, N.J. Nielsen, Optimizing gradient conditions in online comprehensive two-dimensional reversed-phase liquid chromatography by use of the linear solvent strength model, J. Sep. Sci. 40 (2017) 3612–3620.
[3] C.J. Venkatramani, M. Al-Sayah, G. Li, M. Goel, J. Girotti, L. Zang, L. Wigman, P. Yehl, N. Chetwyn, Simultaneous achiral-chiral analysis of pharmaceutical compounds using two-dimensional reversed phase liquid chromatography-supercritical fluid chromatography, Talanta 148 (2016) 548–555.
[4] A.F.G. Gargano, J.B. Shaw, M. Zhou, C.S. Wilkins, T.L. Fillmore, R.J. Moore, G.W. Somsen, L. Paša-Tolić, Increasing the separation capacity of intact histone proteoforms chromatography coupling online weak cation exchange-HILIC to reversed phase LC UVPD-HRMS, J. Proteome Res. 17 (2018) 3791–3800.
[5] P. Yang, L. Bai, W. Wang, J. Rabasco, Analysis of hydrophobically modified ethylene oxide urethane rheology modifiers by comprehensive two dimensional liquid chromatography, J. Chromatogr. A 1560 (2018) 55–62.
[6] P. Venter, M. Muller, J. Vestner, M.A. Stander, A.G.J. Tredoux, H. Pasch, A. de Villiers, Comprehensive three-dimensional LC × LC × ion mobility spectrometry separation combined with high-resolution MS for the analysis of complex samples, Anal. Chem. 90 (2018) 11643–11650.

[7] F. Zhang, Y. Ni, Y. Yuan, W. Yin, Y. Gao, Early urinary candidate biomarker discovery in a rat thioacetamide-induced liver fibrosis model, Sci. China Life Sci. 61 (2018) 1369–1381.
[8] T. Zhou, S. Han, Z. Li, P. He, Purification and quantification of Kunitz Trypsin inhibitor in soybean using two-dimensional liquid chromatography, Food Anal Methods 10 (2017) 3350–3360.
[9] M. Navarro-Reig, J. Jaumot, T.A. van Beek, G. Vivó-Truyols, R. Tauler, Chemometric analysis of comprehensive LC×LC-MS data: resolution of triacylglycerol structural isomers in corn oil, Talanta 160 (2016) 624–635.
[10] H. Gu, Y. Huang, M. Filgueira, P.W. Carr, Effect of first dimension phase selectivity in online comprehensive two dimensional liquid chromatography (LC×LC), J. Chromatogr. A 1218 (2011) 6675–6687.
[11] S. Stephan, C. Jakob, J. Hippler, O.J. Schmitz, A novel four-dimensional analytical approach for analysis of complex samples, Anal Bioanal Chem 408 (2016) 3751–3759.
[12] E. Fornells, B. Barnett, M. Bailey, E.F. Hilder, R.A. Shellie, M.C. Breadmore, Evaporative membrane modulation for comprehensive two-dimensional liquid chromatography, Anal. Chim. Acta 1000 (2018) 303–309.
[13] C.-l. Yao, W.-z. Yang, W. Si, Y. Shen, N.-x. Zhang, H.-l. Chen, H.-q. Pan, M. Yang, W.-y. Wu, D.-a. Guo, An enhanced targeted identification strategy for the selective identification of flavonoid O-glycosides from Carthamus tinctorius by integrating offline two-dimensional liquid chromatography/linear ion-trap-Orbitrap mass spectrometry, high-resolution diagnostic product ions/neutral loss filtering and liquid chromatography-solid phase extraction-nuclear magnetic resonance, J. Chromatogr. A 1491 (2017) 87–97.
[14] B.W.J. Pirok, A.F.G. Gargano, P.J. Schoenmakers, Optimizing separations in online comprehensive two-dimensional liquid chromatography, J. Sep. Sci. 41 (2018) 68–98.
[15] J.C. Giddings, Two-dimensional separations: concept and promise., Anal. Chem. 56 (1984) 1258–1270.
[16] J.C. Giddings, Concepts and comparisons in multidimensional separation, J. High Resolut. Chromatogr. 10 (1987) 319–323.
[17] P. Dugo, F. Cacciola, T. Kumm, G. Dugo, L. Mondello, Comprehensive multidimensional liquid chromatography: theory and applications, J. Chromatogr. A 1184 (2008) 353–368.
[18] H. Cortes, W. Winniford, J. Luong, M. Pursch, Comprehensive two dimensional gas chromatography review, J. Sep. Sci. 32 (2009) 883–904.
[19] F. Cacciola, P. Jandera, Z. Hajdú, P. Česla, L. Mondello, Comprehensive two-dimensional liquid chromatography with parallel gradients for separation of phenolic and flavone antioxidants, J. Chromatogr. A 1149 (2007) 73–87.
[20] P. Jandera, P. Česla, T. Hájek, G. Vohralík, K. Vyňuchalová, J. Fischer, Optimization of separation in two-dimensional high-performance liquid chromatography by adjusting phase system selectivity and using programmed elution techniques, J. Chromatogr. A 1189 (2008) 207–220.
[21] P. Česla, T. Hájek, P. Jandera, Optimization of two-dimensional gradient liquid chromatography separations, J. Chromatogr. A 1216 (2009) 3443–3457.
[22] F. Bedani, W.T. Kok, H.-.G. Janssen, Optimal gradient operation in comprehensive liquid chromatography×liquid chromatography systems with limited orthogonality, Anal. Chim. Acta 654 (2009) 77–84.
[23] D. Li, O.J. Schmitz, Use of shift gradient in the second dimension to improve the separation space in comprehensive two-dimensional liquid chromatography, Anal. Bioanal. Chem. 405 (2013) 6511–6517.
[24] C.J. Venkatramani, S.R. Huang, M. Al-Sayah, I. Patel, L. Wigman, High-resolution two-dimensional liquid chromatography analysis of key linker drug intermediate used in antibody drug conjugates, J. Chromatogr. A 1521 (2017) 63–72.
[25] J. Wang, S. Zheng, Y. Xu, H. Hu, M. Shen, L. Tang, Development of a novel HPLC method for the determination of the impurities in desonide cream and characterization of its impurities by 2D LC-IT-TOF MS, J. Pharm. Biomed. Anal. 161 (2018) 399–406.
[26] J. Wang, Y. Xu, Y. Zhang, H. Wang, W. Zhong, Separation and characterization of unknown impurities in cefonicid sodium by trap-free two-dimensional liquid chromatography combined with ion trap time-of-flight mass spectrometry, Rapid Commun. Mass Spectrom. 31 (2017) 1541–1550.
[27] B.W.J. Pirok, D.R. Stoll, P.J. Schoenmakers, Recent developments in two-dimensional liquid chromatography: fundamental improvements for practical applications, Anal. Chem. 91 (2019) 240–263.
[28] G.M. Leme, F. Cacciola, P. Donato, A.J. Cavalheiro, P. Dugo, L. Mondello, Continuous vs. segmented second-dimension system gradients for comprehensive two-dimensional liquid chromatography of sugarcane (Saccharum spp.), Anal. Bioanal. Chem. 406 (2014) 4315–4324.
[29] R. Dück, H. Sonderfeld, O.J. Schmitz, A simple method for the determination of peak distribution in comprehensive two-dimensional liquid chromatography, J. Chromatogr. A 1246 (2012) 69–75.
[30] G. Semard, V. Peulon-Agasse, A. Bruchet, J.-.P. Bouillon, P. Cardinaël, Convex hull, A new method to determine the separation space used and to optimize operating conditions for comprehensive two-dimensional gas chromatography, J. Chromatogr. A 1217 (2010) 5449–5454.
[31] M. Camenzuli, P.J. Schoenmakers, A new measure of orthogonality for multi-dimensional chromatography, Anal. Chim. Acta 838 (2014) 93–101.
[32] C.M. Willemse, M.A. Stander, J. Vestner, A.G.J. Tredoux, A. de Villiers, Comprehensive two-dimensional hydrophilic interaction chromatography (HILIC) × reversed-phase liquid chromatography coupled to high-resolution mass spectrometry (RP-LC-UV-MS) analysis of anthocyanins and derived pigments in red wine, Anal. Chem. 87 (2015) 12006–12015.
[33] B.W.J. Pirok, S. Pous-Torres, C. Ortiz-Bolsico, G. Vivó-Truyols, P.J. Schoenmakers, Program for the interpretive optimization of two-dimensional resolution, J. Chromatogr. A 1450 (2016) 29–37.
[34] M.R. Schure, Quantification of resolution for two-dimensional separations, J. Microcolumn Sep. 9 (1997) 169–176.
[35] M. Hadjmohammadi, V. Sharifi, Simultaneous optimization of the resolution and analysis time of flavonoids in reverse phase liquid chromatography using Derringer's desirability function, J. Chromatogr. B 880 (2012) 34–41.
[36] K. Kamel, M.R. Hadjmohammadi, Application of multilinear gradient elution for optimization of separation of chlorophenols using Derringer's desirability function, Chromatographia 67 (2008) 169–172.
[37] B. Bourguignon, D.L. Massart, Simultaneous optimization of several chromatographic performance goals using Derringer's desirability function, J. Chromatogr. A 586 (1991) 11–20.
[38] A. D'Attoma, C. Grivel, S. Heinisch, On-line comprehensive two-dimensional separations of charged compounds using reversed-phase high performance liquid chromatography and hydrophilic interaction chromatography. Part I: orthogonality and practical peak capacity considerations, J. Chromatogr. A 1262 (2012) 148–159.
[39] S.C. Rutan, J.M. Davis, P.W. Carr, Fractional coverage metrics based on ecological home range for calculation of the effective peak capacity in comprehensive two-dimensional separations, J. Chromatogr. A 1255 (2012) 267–276.
[40] X. Li, D.R. Stoll, P.W. Carr, Equation for peak capacity estimation in two-dimensional liquid chromatography, Anal. Chem. 81 (2009) 845–850.